CEAS Aeronautical Journal
https://doi.org/10.1007/s13272-025-00822-5

SHORT COMMUNICATION

Airborne SARS-CoV-2 in aircraft cabins: new inactivation data significantly influences infection risk predictions

Florian Webner[1,2] · Andrei Shishkin[1] · Daniel Schmeling[1] · Claus Wagner[1,2]

Received: 8 January 2025 / Revised: 3 February 2025 / Accepted: 10 February 2025

Abstract
We predict the SARS-CoV-2 infection risk in aircraft cabins by simulating the aerosol transport with computational fluid dynamics and taking medical parameters into account. A recently presented new measurement technique allows us to measure the rapid virus inactivation after exhalation with high temporal resolution. In addition, much higher airborne SARS-CoV-2 inactivation rates than in previous studies were obtained. This raises the question of how the new knowledge of SARS-CoV-2 stability affects the prediction of infection risk. To answer this question, we evaluated 70 Lagrangian particle simulations with an index person sitting in all possible seats in an aircraft cabin. We then estimated the infection risk for the other passengers based on the old and new SARS-CoV-2 stability data. For typical transmission events, we found that the predicted infection risk is reduced by about 50% for the new stability data at low CO_2 (500 ppm). However, elevated ambient CO_2 concentrations of 3000 ppm protect the virus from inactivation and increase infection risk by about 50% compared to low CO_2. In addition, a high relative humidity of the ambient air, e.g., from exhaled breath, delays the rapid inactivation by a few seconds, increasing the risk of infection for immediate neighbors.

1 Introduction

Previous publications have reported airborne SARS-CoV-2 half-lives of 1.1 hours [1], 16 hours [2], or 1.9 hours [3]. This means that more than 98 % of viruses remain active during particle transport in an aircraft cabin, so that airborne inactivation can be neglected [4]. However, using a new measurement technique with a high temporal resolution, Haddrell et al. (2024) [5] observed a 50 % loss of airborne SARS-CoV-2 infectivity within half a minute. In the present study, we follow their suggestion (quoting [5]): 'In the future, the effect the rapid loss of infectivity in the aerosol phase at low RH [relative humidity] has on short-distance transmission risk should be explored using a CFD [computational fluid dynamics] model.'.

While many infection risk models do not account for virus inactivation during particle transport [6], we have recently introduced an infection risk model based on CFD particle predictions, that is capable of accounting for airborne virus inactivation of individual particles [4]. In the present study, we report the comparison of the estimated infection risk in the cabin of the Dornier 728 (Do728) regional aircraft with the SARS-CoV-2 inactivation rates obtained using "traditional measurement" (rotating drum) [3] and controlled electrodynamic levitation and extraction of bioaerosols onto a substrate (CELEBS) [5, 7]. Since CO_2 concentrations are typically elevated in aircraft cabins, we include the investigation of the influence of CO_2-dependent viral stability measured by [5] on infection risk. To the best of our knowledge, the results of Haddrell et al. have not been reproduced by another independent research team yet.

2 Methods

We solve the unsteady Reynolds-averaged Navier-Stokes (URANS) equations to predict the airflows in the fully occupied Do728 cabin, with 14 rows of seats, five seats in each row, and with 70 simulated dummies, each given skin temperature and clothing thermal conductivity. We use a standard mixed ventilation, with 10 liters of fresh air per second per person (700 l/s in total) supplied from the side walls above and below the overhead luggage compartments. We

✉ Florian Webner
Florian.Webner@dlr.de

[1] Institute of Aerodynamics and Flow Technology, German Aerospace Center (DLR), 37073 Göttingen, Germany

[2] Institute of Thermodynamics and Fluid Mechanics, Technische Universität Ilmenau, 98693 Ilmenau, Germany

Published online: 05 March 2025

assume 100 % efficient particle filters, i. e., no particles re-enter the cabin with the fresh air supply. The exhaust vents are located on the side walls near the floor. A particle cloud is then seeded into the time-averaged velocity field and the subsequent particle motion is predicted with the Lagrangian solver for 600 s. More details on the URANS/Lagrangian approach and its validation against experimental measurements can be found in Schmeling et al. [8] and Shishkin et al. [9]. To estimate the risk of infection, we created a standard case in [4] with the parameters shown in Table 1. To improve the stochastic reliability of the particle analysis, 10^5 particles were seeded into the CFD domain.

In addition, we used the following four different inactivation rates: the original strain at 20 % RH (unknown CO_2 concentration) measured with a rotating drum by Dabisch et al. [3], the original strain and Delta strain at 40 % RH and 500 ppm ambient CO_2, and the inactivation rate of the Delta strain at 90 % RH measured with CELEBS at 500 ppm and 3000 ppm ambient CO_2 [5, 7]. The infection risk is then estimated based on a human challenge study [10] in which 34 volunteers were exposed to a SARS-CoV-2 dose of 10 $TCID_{50}$ in a controlled environment, as discussed in Webner et al. [4].

A total of 70 CFD simuations are performed which differed in the seat position of the index person (IP) occupying any possible seat. The individual infection risks and virus stabilities predicted in these 70 simulations are averaged to obtain a mean infection risk.

3 Results & discussion

In Fig. 1 the predicted mean infection risk is written over each seat written in bold above the mean stability weighted by particle concentration. In addition, the infection risk and virus stability are averaged over the seat columns and written on the right-hand side of the figure. The figure shows four seat maps for four different inactivation rates.

For the inactivation rate of Dabisch et al. [3], which we also used in [4], the figure shows that when sitting on 14E, the infection risk averaged over all 69 other positions of the index person (based on the standard case introduced in Table 1) equals 0.5 % and 98.5 % of the viruses remain active during the transport until inhalation. This is the lowest virus stability for this inactivation rate, indicating that airborne inactivation is insignificant. Although the virus stability on all seats is similar (≈ 99 %), the infection risk varies: Window seats pose reduced infection risks. This is due to the large-scale circulations that moves air from the windows to the aisle at face level, then down to the floor and back to the sidewalls near the floor. We discussed this effect in more detail in [11]. In brief: The large-scale circulations carry particles exhaled by the passengers in window seats directly to their neighbors. This increases the infection risk on the aisle seats. In addition, the risk is higher on the three-person bench (C, D, E) than on the two-person bench (A, B), because there are more potentially infected neighbors.

Considering the original strain at 40 % RH and 500 ppm CO_2, the lowest virus stability of 38.8 % is still found at 14E - a significant reduction in the inhaled infectious dose. The predicted infection risk is only about half of what we estimated based on the inactivation rate previously used for all seats. Although there are local differences in viral stability, the local differences in infection risk are dominated by the local differences in particle concentrations caused by the large-scale circulations as discussed above.

For the Delta strain at 90% RH and 500 ppm CO_2, we obtain strong differences between the seat columns: The average stability in column E is only 45.4 % compared to 68.8 % in column B. Due to the high temporal resolution in the inactivation curves measured by Haddrell et al. [7], the following insights were obtained: For the original strain at 40 % RH, the stability drops to about 50 % almost immediately after exhalation, whereas for the Delta strain at 90 % RH, this rapid inactivation is delayed by a few seconds. Therefore, more active particles reach the immediate neighbors (downstream), increasing virus stability on all seats, but to a lesser extent at the window seats (upstream). The local differences in virus stability are significant and increase the average infection risk from 0.5 % to 0.7 % on columns C and D, while having no significant effect on window seats. Compared to the original strain at lower (40 %) RH, this also increases the relative difference of infection risk between columns A and C to 0.2 % and 0.7 %, respectively. While air in an aircraft is typically dry, the RH of exhaled air is significantly higher. Since the inactivation rates for low and high RH differ mainly in the first few seconds, as particles float in the exhaled humid puff, in most cases the inactivation at high RH may be more accurate, even if the ambient air is dry.

For the Delta strain at 90 % RH and elevated ambient CO_2 (3000 ppm), the virus stability and the infection risk are significantly increased on all seats. This underlines the findings of Haddrell et al. [5] that CO_2 directly affects infection risk by protecting the virus from inactivation. Again, the CO_2 concentration in the immediate vicinity of the particles is highest immediately after exhalation (up to 50,000 ppm), as the particles float in the CO_2-rich exhaled air. As the exhaled

Table 1 Parameters in the standard case

Quantity	Virus emission rate	Fraction of active virus	Pulmonary inhalation rate	Exposure time
Symbol/unit	$\dot{R}I\frac{RNA}{s}$	$fI\frac{TCID_{50}}{RNA}$	$p_{in}\,I\frac{liter}{min}$	t/min
Value	500	10^{-4}	6	120

Fig. 1 Infection risk written in bold and virus stability averaged over 70 possible seat locations of the index person on all seats for four different inactivation rates. Seat column averages are shown on the right hand side

air mixes with ambient air, the CO_2 concentration is reduced to ambient levels over time. Therefore, for the most accurate modeling, experimental measurements of the virus inactivation at time-dependent RH and CO_2 corresponding to human exhalation would be required.

Figure 2a shows the number of expected infections over D/D_{sc}, where D is any arbitrary inhaled infectious dose and D_{sc} is the inhaled infectious dose of the standard case (see Table 1). This allows the number of expected infections to be estimated with parameters different from those

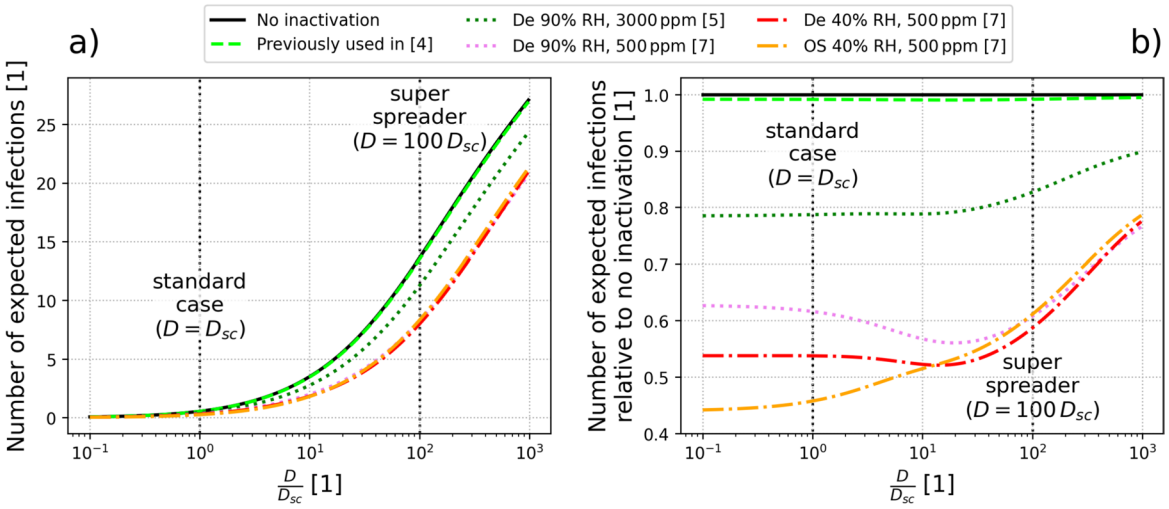

Fig. 2 Number of expected infections (**a**) and number of expected infections relative to no inactivation (**b**) over $\frac{D}{D_{sc}}$ for different virus inactivation rates for the original strain (OS) and Delta strain (De) at different RHs and CO_2 concentrations

in Table 1 (D is proportional to the product $\dot{R}fp_{in}t$). The expected infections are shown for the different inactivation curves.

For the standard case ($\frac{D}{D_{sc}} = 1$), which is based on parameter values found in the literature, the number of expected infections is low ($\approx 0.25 - 0.5$). However, higher virus emission rates, higher fractions of active virus, and longer flight times are possible (discussed in detail in [4]). Therefore, we also consider a super-spreader case with $\frac{D}{D_{sc}} = 100$, for which nearly 14 infections are predicted with the inactivation used in [4]. In contrast, considering the inactivation rates at 500 and 3000 ppm CO_2 measured by Haddrell et al. leads to approximately 8 and 11 infections, respectively. The plot also shows that the absolute differences obtained for the considered cases are almost constant for increasing $\frac{D}{D_{sc}}$.

Figure 2b shows the relative number of expected infections compared to the case with no airborne inactivation. In the standard case, the number of expected infections for the original strain is only 46 % compared to no inactivation. For the Delta strain at 500 ppm CO_2 concentration, this increases to 53 % at low RH and 61 % at high RH. At elevated CO_2 (3000 ppm), the relative number of expected infections increases further to 78 %. In the case of a superspreader, the inactivation curves for low CO_2 become similar.

This is because the inactivation rates differ mainly in the first few seconds after exhalation, which means that the difference mainly affects close neighbors with low particle travel times. The close neighbors are also exposed to the highest particle concentrations. Therefore, as the dose increases, the close neighbors are the first to reach ≈100% infection risk. Since the initial difference in the inactivation curves mainly affects close neighbors, the difference becomes irrelevant, when the close neighbors reach ≈ 100% infection risk.

Table 2 summarizes the key results.

4 Conclusions

Based on the evaluations discussed above, we draw the following conclusions for SARS-CoV-2 transmission in a Do728 aircraft:

Table 2 Summary of the key results for the standard case (SC) and the superspreader case (SSC)—with a 100 times higher inhaled dose than SC—for the original strain (OS) and Delta strain (De)

	Mean/min stability [%]	Mean/max infection risk [%]		Expected number of secondary infections [1]	
	SC	SC	SSC	SC	SSC
No inactivation	100/100	0.78/1.65	19.7/28.7	0.54	13.6
[3] previously used in [4]	99.1 /98.5	0.77/1.64	19.6/28.5	0.53	13.5
OS low RH, low CO_2 [7]	43.4/38.8	0.36/0.80	12.1/18.6	0.25	8.3
De low RH, low CO_2 [7]	50.1/36.5	0.42/1.00	11.6/17.9	0.29	8.0
De high RH, low CO_2 [7]	59.0/39.6	0.48/1.21	12.0/18.3	0.33	8.3
De high RH, high CO_2 [5]	77.2/69.6	0.61/1.34	16.3/24.1	0.42	11.3

"Min" and "Max"refer to the minimum and maximum values averaged over the 70 possible seats of the index person, respectively, while "Mean" refers to the values averaged over all 70 times 69 possible seat combinations of the index person and the susceptible person

- We revise our previous conclusion in [4] that airborne inactivation can be neglected: Using the inactivation data measured by Haddrell et al. has significant impact on the predicted infection risk.
- In average, the delayed rapid inactivation of the Delta strain at high RH (90 %) and low CO_2 (500 ppm) results in higher virus stability when reaching passengers downstream of the index person (especially in columns B, C, and D), and thus an overall 33 % higher infection risk compared to the original strain under the same environmental conditions.
- For a "typical" index person (standard case), the inactivation data measured by Haddrell et al. at low ambient CO_2 concentrations is expected to result in about half as many infections (46 % to 61 %) as no inactivation or "traditional" inactivation data. For a super-spreading event, about 5 fewer infections are expected with the Haddrell et al. data.
- Elevated CO_2 (3000 ppm) significantly increases infection risk, resulting in about 3 additional expected infections for superspreaders or about 50 % more infections for a "typical" transmission event.

Acknowledgements This work was funded by the DLR project GANDALF. The authors gratefully acknowledge the scientific support and HPC resources provided by the German Aerospace Center (DLR). The HPC system CARO is partially funded by "Ministry of Science and Culture of Lower Saxony" and "Federal Ministry for Economic Affairs and Climate Action".

Author contributions F.W. developed the concept, evaluated the data, prepared the figures and wrote the original draft. A.S. generated the raw data (CFD). D.S. and C.W. supervised and were also involved in the concept development. All authors reviewed the manuscript.

Funding Open Access funding enabled and organized by Projekt DEAL.

Data availability Please contact the corresponding author for data and materials upon reasonable requests.

Declarations

Conflict of interest The authors declare no competing interests.

References

1. van Doremalen, N., Bushmaker, T., Morris, D.H., Holbrook, M.G., Gamble, A., Williamson, B.N., Tamin, A., Harcourt, J.L., Thornburg, N.J., Gerber, S.I., Lloyd-Smith, J.O., de Wit, E., Munster, V.J.: Aerosol and surface stability of sars-cov-2 as compared with sars-cov-1. N. Engl. J. Med. **382**(16), 1564–1567 (2020). https://doi.org/10.1056/NEJMc2004973
2. Fears, A.C., Klimstra, W.B., Duprex, P., Hartman, A., Weaver, S.C., Plante, K.S., Mirchandani, D., Plante, J.A., Aguilar, P.V., FernÃndez, D., Nalca, A., Totura, A., Dyer, D., Kearney, B., Lackemeyer, M., Bohannon, J.K., Johnson, R., Garry, R.F., Reed, D.S., Roy, C.J.: Persistence of severe acute respiratory syndrome coronavirus 2 in aerosol suspensions. Emerg. Infect. Dis. **26**(9), 2168–2171 (2020). https://doi.org/10.3201/eid2609.201806
3. Dabisch, P., Schuit, M., Herzog, A., Beck, K., Wood, S., Krause, M., Miller, D., Weaver, W., Freeburger, D., Hooper, I., Green, B., Williams, G., Holland, B., Bohannon, J., Wahl, V., Yolitz, J., Hevey, M., Ratnesar-Shumate, S.: The influence of temperature, humidity, and simulated sunlight on the infectivity of sars-cov-2 in aerosols. Aerosol Sci. Technol. **55**(2), 142–153 (2020). https://doi.org/10.1080/02786826.2020.1829536
4. Webner, F., Shishkin, A., Schmeling, D., Wagner, C.: A direct infection risk model for cfd predictions and its application to sars-cov-2 aircraft cabin transmission. Indoor Air **2024**, 1–18 (2024). https://doi.org/10.1155/2024/9927275
5. Haddrell, A., Oswin, H., Otero-Fernandez, M., Robinson, J.F., Cogan, T., Alexander, R., Mann, J.F.S., Hill, D., Finn, A., Davidson, A.D., Reid, J.P.: Ambient carbon dioxide concentration correlates with sars-cov-2 aerostability and infection risk. Nat. Commun. (2024). https://doi.org/10.1038/s41467-024-47777-5
6. Pourfattah, F., Wang, L.-P., Deng, W., Ma, Y.-F., Hu, L., Yang, B.: Challenges in simulating and modeling the airborne virus transmission: a state-of-the-art review. Phys. Fluids (2021). https://doi.org/10.1063/5.0061469
7. Haddrell, A., Otero-Fernandez, M., Oswin, H., Cogan, T., Bazire, J., Tian, J., Alexander, R., Mann, J.F.S., Hill, D., Finn, A., Davidson, A.D., Reid, J.P.: Differences in airborne stability of sars-cov-2 variants of concern is impacted by alkalinity of surrogates of respiratory aerosol. J. R. Soc. Interface (2023). https://doi.org/10.1098/rsif.2023.0062
8. Schmeling, D., Shishkin, A., Schiepel, D., Wagner, C.: Numerical and experimental study of aerosol dispersion in the do728 aircraft cabin. CEAS Aeronaut. J. **14**(2), 509–526 (2023). https://doi.org/10.1007/s13272-023-00644-3
9. Shishkin, A., Schiepel, D., Schmeling, D.: Numerical study ofÂ aerosol dispersion inÂ theÂ aircraft cabin. In: Dillmann, A., Heller, G., Krämer, E., Wagner, C., Weiss, J. (eds.) New Results in Numerical and Experimental Fluid Mechanics XIV, pp. 549–558. Springer Nature Switzerland, Cham (2024)
10. Killingley, B., Mann, A.J., Kalinova, M., Boyers, A., Goonawardane, N., Zhou, J., Lindsell, K., Hare, S.S., Brown, J., Frise, R., Smith, E., Hopkins, C., Noulin, N., Löndt, B., Wilkinson, T., Harden, S., McShane, H., Baillet, M., Gilbert, A., Jacobs, M., Charman, C., Mande, P., Nguyen-Van-Tam, J.S., Semple, M.G., Read, R.C., Ferguson, N.M., Openshaw, P.J., Rapeport, G., Barclay, W.S., Catchpole, A.P., Chiu, C.: Safety, tolerability and viral kinetics during sars-cov-2 human challenge in young adults. Nat. Med. **28**(5), 1031–1041 (2022). https://doi.org/10.1038/s41591-022-01780-9
11. Webner, F., Shishkin, A., Schmeling, D., Wagner, C.: Identifying the safest in aircraft: Modelling infection risk for 70 different source locations, 18th International Conference on Indoor Air Quality and Climate (Indoor Air 2024), ISIAQ, Honolulu,

HI, USA, pp. 646–653 (2025). https://www.scopus.com/inward/record.uri?eid=2-s2.0-85210883420&partnerID=40&md5=52b8c45e606c3dab3ce00a3733cd1c38.